

One Terahertz Full-Field Digital Back-Propagation over 3000 km

Eric Sillekens^(1,†), Ruben S. Luis⁽²⁾, Giammarco Di Sciullo⁽³⁾, Robert Emmerich⁽⁴⁾, Carlo Centofanti⁽³⁾, Daniele Orsuti⁽⁵⁾, Robson A. Colares⁽⁶⁾, Mindaugas Jarmolovičius⁽¹⁾, Ronit Sohanpal⁽¹⁾, Darli A. A. Melo⁽⁶⁾, Luca Palmieri⁽⁵⁾, Colja Schubert⁽⁴⁾, Ronald Freund⁽⁴⁾, Cristian Antonelli⁽³⁾, Robert I. Killey⁽¹⁾, Polina Bayvel⁽¹⁾, and Hideaki Furukawa⁽²⁾

⁽¹⁾ Optical Networks Group, UCL (University College London), Gower Street, London, WC1E 6BT, UK

⁽²⁾ NICT, Nukui Kitamachi 4-2-1, Koganei, 184-8795 Tokyo, Japan

⁽³⁾ Università degli Studi dell'Aquila, 67100, L'Aquila, Italy

⁽⁴⁾ Fraunhofer Heinrich-Hertz-Institut, Einsteinufer 37, 10587 Berlin, Germany

⁽⁵⁾ Università degli Studi di Padova, Via G. Gradenigo 6/B, 35131, Padova, Italy

⁽⁶⁾ Universidade Estadual de Campinas (Unicamp), Campinas, SP, 13083-859, Brazil

^(†) e.sillekens@ucl.ac.uk

Abstract We implement full-field digital back-propagation with a 1-THz receiver using 20 synchronous frequency-adjacent coherent receivers with digital stitching and a frequency-comb local oscillator. Relative to electronic dispersion compensation, per-channel DBP and full-field DBP achieve throughput gains of 2.2% and 5.4%, respectively. ©2026 The Author(s)

Introduction

Full-field digital back-propagation (DBP) is the process by which all interfering signals in a transmission link are jointly detected and incorporated into a wideband DBP computation [1]. This allows the compensation of inter-channel fibre nonlinearities, such as cross-phase modulation and four-wave mixing, leading to higher nonlinearity-compensation gains [2, 3]. In order to capture a wideband spectrum, it may be necessary to frequency-stitch signals detected by multiple synchronous coherent receivers, as shown in [4–9]. It may also be necessary to use frequency comb as local oscillator, in order to achieve a consistent frequency spacing between receivers or transmitters [10]. At sufficiently wide bandwidths, third-order dispersion (β_3) must also be included in the propagation model, since the dispersion slope across 1 THz amounts to the equivalent of more than

100 km of dispersion after 3000 km of fibre [11]. Nevertheless, the gain of full-field DBP may be fundamentally limited by phenomena such as noise [12] or polarisation-mode dispersion [13]. As such, further research is required to evaluate the potential of this approach to support long-distance transmission.

In this work, we demonstrate full-field 1-THz DBP on a 20×47.5 GBd, 50-GHz-spaced, PM-64QAM WDM signal after transmission through a 3000-km straight-line pure-silica-core G.654 fibre link. The full-field receiver is implemented using 20 synchronous coherent receivers, each with 36 GHz electrical bandwidth and 11 GHz overlap for coherent stitching, and 50-GHz-spaced coherent laser lines from an optical frequency comb as local oscillators. Full-field DBP achieved a 393-Gbps (5.4%) gain over EDC, more than twice the 160-Gbps (2.2%) gain achieved by per-channel

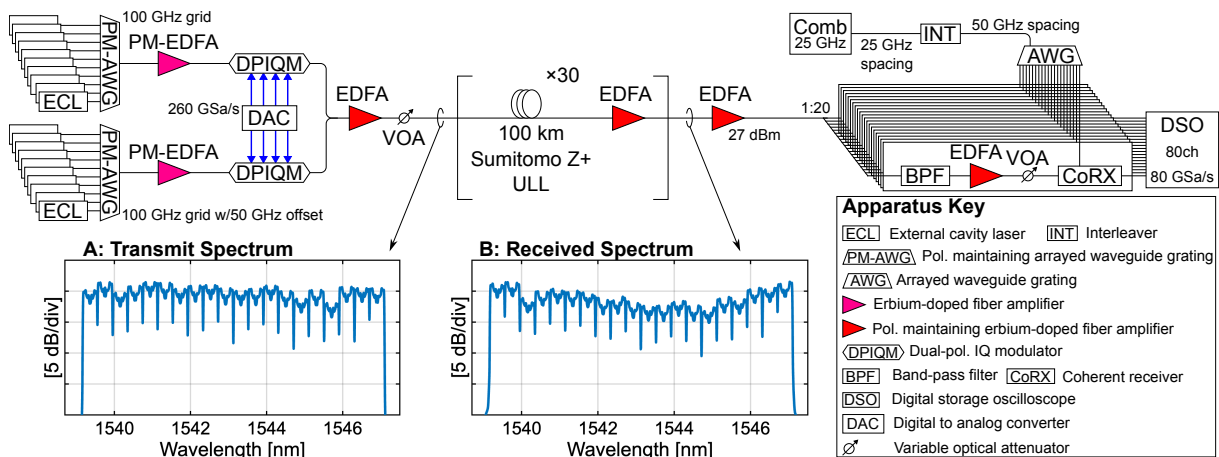


Fig. 1: Experimental setup for the 1-THz full-field DBP demonstration. Two DPIQMs are used to modulate odd and even channels, which are then combined and launched into the straight-line link. At the receiver, the signal is split into 20 branches, each of which is filtered and fed into a coherent receiver, with filtered lines from a comb used as local oscillators. The transmitted and received spectra are shown in insets (A) and (B), respectively.

DBP.

Experimental Transmission Setup

A diagram of the experimental setup is shown in Figure 1. At the transmitter, 20 free-running external-cavity lasers (ECLs) with linewidths below 100 kHz were separated into odd and even sub-bands and combined using two 100-GHz arrayed-waveguide gratings (AWGs) with a relative 50-GHz offset. Each group of sub-bands was modulated independently using a dual-polarisation in-phase/quadrature modulator (DPIQM), after which the two groups were recombined with a 3-dB coupler and amplified by an erbium-doped fibre amplifier (EDFA) before launch into the link.

Each channel was modulated using 64-QAM at a symbol rate of 47.5 GBd. The channels were spaced 50 GHz apart. The symbols were root-raised-cosine (RRC) shaped with a roll-off factor of 0.01. Transmitter compensation was applied, and the resulting waveforms were upsampled and loaded into a digital-to-analogue converter (DAC) with a sampling rate of 260 GSa/s.

The transmission link consisted of 30 spans of 100 km of pure-silica-core G.654 fibre, with a gain-flattening EDFA following each span to compensate the span loss and equalise the spectral power profile.

At the receiver, the signal was boosted by an EDFA to 27 dBm output power. The amplified signal was then divided into 20 branches using a power splitter; each branch passed through a narrowband bandpass filter, was amplified, and was fed into one of 20 dual-polarisation coherent receivers with 70-GHz photodiodes. The 80-channel, 80-GSa/s digital storage oscilloscope (DSO) with 36-GHz electrical bandwidth digitised the signal for offline processing. For the local oscillator (LO), a 25-GHz-spaced optical frequency comb with an interleaver (INT) and a 50-GHz-spaced AWG routed a single comb line to each of the 20 coherent receivers.

Frequency Stitched Receiver

The 20 received sub-bands were first time-aligned using the overlap between adjacent sub-bands. The relative delay was estimated from the total received power, $|E_x|^2 + |E_y|^2$, which is insensitive to the inter-sub-band frequency offset. A coarse estimate was used to determine the integer-sample delay, followed by a fine estimate of the fractional delay from a linear phase ramp in the frequency domain. The adjacent sub-bands were then frequency-aligned by estimating the inter-sub-band spacing from the overlap region. This sub-picosecond timing alignment and sub-kHz frequency alignment were necessary to achieve a measurable full-field DBP gain. After time and frequency alignment, the sub-bands were stitched

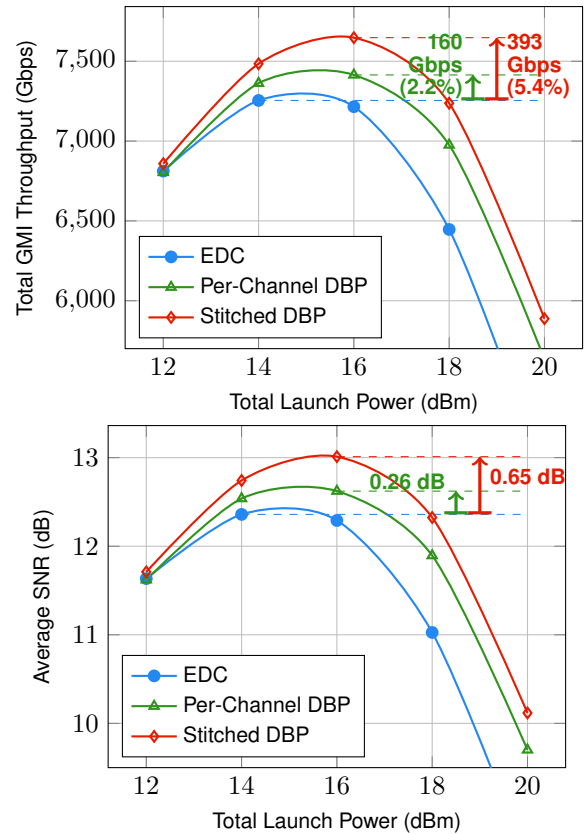


Fig. 2: Total GMI throughput (top) and average SNR (bottom) vs. total launch power for EDC, per-channel DBP, and full-field stitched DBP after 3000 km transmission.

together to reconstruct the full 1-THz field, using raised-cosine weighting at the sub-band edges to smooth the transitions.

The DBP algorithm¹ was implemented using the split-step Fourier method (SSFM) to numerically solve the inverse Manakov equation [1, 14]. The step size was chosen using adaptive local-error control following Sinkin et al. [15], with a target local error of 5×10^{-9} . Full-field DBP was performed at a sampling rate of 4 THz, while per-channel DBP used a 200-GHz sampling rate. The propagation model included both β_2 and β_3 , estimated from the EDC stage: β_2 was obtained on a per-channel basis using the CMA-based dispersion estimate [16, Eq. (3)], and β_3 was obtained from a linear regression across the 20 channels. The resulting fibre parameters were $D = 20.1955$ ps/(nm·km) and $S = 0.0628$ ps/(nm²·km) at the reference wavelength $\lambda_{\text{ref}} = 1543.13$ nm, taken as the centre of the 10 channel pairs. A parameter sweep for the 16-dBm result was used to determine the nonlinear coefficient $\gamma_{\text{DBP}} = 0.45$ /W/km and a fibre loss of $\alpha_{\text{DBP}} = 0.154$ dB/km.

For data recovery, the back-propagated signal was retimed to 2 samples/symbol, followed by LO carrier-frequency-offset removal. A data-aided

¹https://github.com/zceemja/labathon_ecoc2025/blob/12008e7e0aaca1b58ddc83505e010f9b2a82568e/functions.py#L56

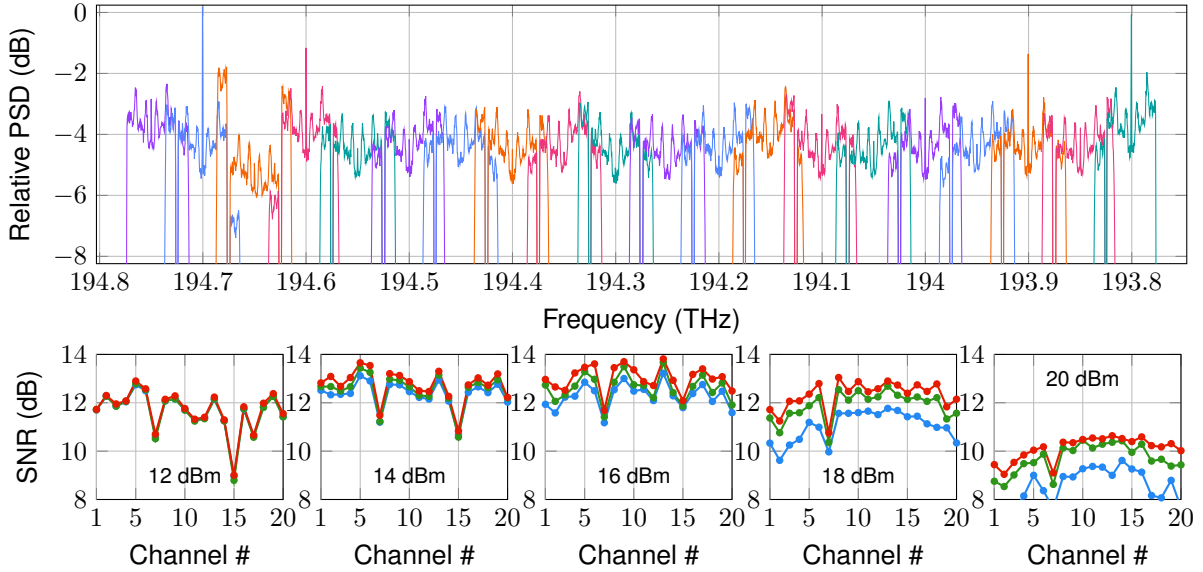


Fig. 3: Top: received optical spectrum at 16 dBm launch power. Bottom: per-channel SNR for each of the five launch powers tested (12–20 dBm), comparing EDC (blue), per-channel DBP (green), and full-field stitched DBP (red).

LMS equaliser with carrier recovery in the loop was then applied, followed by a decision-directed LMS equaliser, again with carrier recovery in the loop. Performance was evaluated using the generalised mutual information (GMI).

Results

Figure 2 shows the total GMI throughput and average SNR as a function of total launch power for EDC, per-channel DBP, and full-field stitched DBP. The peak throughput for EDC is 7254.4 Gbps at 14 dBm, for per-channel DBP 7414.3 Gbps at 16 dBm, and for full-field stitched DBP 7647.6 Gbps at 16 dBm. Full-field stitched DBP thus achieves a gain of 393 Gbps (5.4%) over EDC, more than twice the 160 Gbps (2.2%) gain achieved by per-channel DBP. In terms of average SNR, the peak values are 12.36 dB, 12.62 dB, and 13.01 dB for EDC, per-channel DBP, and stitched DBP, respectively, corresponding to gains of 0.65 dB and 0.26 dB for stitched DBP over EDC and per-channel DBP.

Figure 3 shows the reconstructed spectrum at the optimal launch power of 16 dBm at the top, and the per-channel SNR at the bottom for the measured launch powers. The stitched DBP consistently improves the SNR across all 20 channels, with the largest gains observed in channels 1, 4, 6, and 8–10. The average SNR gain over EDC per channel ranges from 0.3 to 1.3 dB at this launch power. As is visible in the received spectrum, the optical power is not uniform across sub-bands, meaning that the effective γP product used in the DBP model is inaccurate on a per-slice basis. A per-slice optimisation of the effective launch power used in the DBP model could reduce this mismatch and further improve the full-field compensation gain. This could be achieved by sweeping

the γP product for each sub-band to maximise the recovered SNR. Furthermore, polarisation-mode dispersion (PMD) causes the field to decorrelate over long distances and limits the achievable gain unless it is explicitly accounted for in the back-propagation model [3, 13].

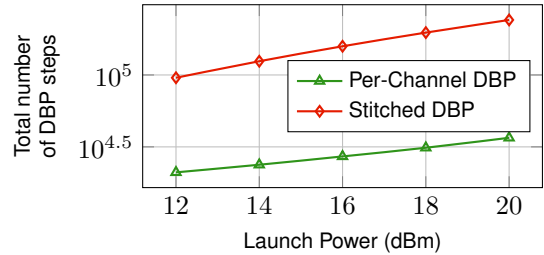


Fig. 4: Number of SSFM steps vs. total launch power for per-channel and full-field stitched DBP.

Figure 4 shows the number of SSFM steps required for convergence as a function of launch power. As expected, the number of steps increases with launch power due to the stronger nonlinearity. Full-field DBP requires approximately $5.8\times$ more steps than all per-channel DBP instances combined. This is on top of the $20\times$ increase in bandwidth.

Conclusion

We have demonstrated full-field digital back-propagation over 3000 km with 1-THz receiver bandwidth, enabled by 20 synchronous coherent receivers, a frequency-comb local oscillator, and a propagation model including dispersion slope. Sub-picosecond timing alignment and sub-kHz frequency alignment between channels were necessary to observe full-field DBP gain. For a 20×47.5 GBd, 50-GHz-spaced, PM-64QAM WDM signal, full-field DBP yielded a 393 Gbps (5.4%) throughput gain over EDC, more than double the 160 Gbps (2.2%) achieved by per-channel DBP.

Acknowledgements

The authors gratefully acknowledge all individuals and organisations that contributed to this research and supported the collaboration. This work was supported in part by the Engineering and Physical Sciences Research Council (EPSRC) under the programme grant “Transforming networks - building an intelligent optical infrastructure (TRANSNET)’ (EP/R035342/1), and “Extremely Wideband Optical Fibre Communication Systems (EWOC)’ (EP/W015714/1), and by the German Federal Ministry of Research, Technology and Space under the CELTIC-NEXT project SUSTAINET-Advance (16KIS2272). Robson A. Colares and Darli A. A. Mello are partially sponsored by CNPq grant #405940/2022-0 and CAPES grant #88887.954253/2024-00. Eric Sillekens’ fellowship titled “Enabling Power Efficient Optical Communication through Novel Digital Signal Processing (EPIC DSP)” was supported by Department for Science, Innovation and Technology and the Royal Academy of Engineering under the Research Fellowships scheme, and Polina Bayvel by a Royal Society Research Professorship.

References

- [1] E. Ip, “Nonlinear Compensation Using Backpropagation for Polarization-Multiplexed Transmission”, *Journal of Lightwave Technology*, vol. 28, no. 6, pp. 939–951, Mar. 2010. DOI: 10.1109/JLT.2010.2040135
- [2] R. Dar and P. J. Winzer, “On the Limits of Digital Back-Propagation in Fully Loaded WDM Systems”, *IEEE Photonics Technology Letters*, vol. 28, no. 11, pp. 1253–1256, Jun. 2016. DOI: 10.1109/LPT.2016.2522969
- [3] K. Goroshko, H. Louchet, and A. Richter, “Fundamental Limitations of Digital Back Propagation due to Polarization Mode Dispersion”, in *Asia Communications and Photonics Conference 2015*, Hong Kong, 2015, ASu3F.5. DOI: 10.1364/ACPC.2015.ASu3F.5
- [4] N. K. Fontaine, G. Raybon, B. Guan, A. Adamiecki, P. J. Winzer, R. Ryf, A. Konczykowska, F. Jorge, J.-Y. Dupuy, L. L. Buhl, S. Chandrashekhar, R. Delbue, P. Pupalaiakis, and A. Sureka, “228-GHz Coherent Receiver using Digital Optical Bandwidth Interleaving and Reception of 214-GBd (856-Gb/s) PDM-QPSK”, in *European Conference and Exhibition on Optical Communication*, Amsterdam, 2012, Th.3.A.1. DOI: 10.1364/ECEOC.2012.Th.3.A.1
- [5] K. Shi, E. Sillekens, and B. C. Thomsen, “246 GHz Digitally Stitched Coherent Receiver”, in *Optical Fiber Communication Conference*, Los Angeles, California, 2017, p. M3D.3. DOI: 10.1364/OFC.2017.M3D.3
- [6] C. Deakin, J. Zang, X. Chen, D. Che, L. Dallachiesa, B. Stern, N. K. Fontaine, and S. Papp, “2.4-thz bandwidth optical coherent receiver based on a photonic crystal microcomb”, in *ECOC*, Frankfurt, Germany, 2024, pp. 766–769.
- [7] D. Drayss, D. Fang, C. Füllner, G. Lihachev, T. Henauer, Y. Chen, H. Peng, P. Marin-Palomo, T. Zwick, W. Freude, T. J. Kippenberg, S. Randel, and C. Koos, “Non-sliced optical arbitrary waveform measurement (OAWM) using soliton microcombs”, *Optica*, vol. 10, no. 7, pp. 888–896, Jul. 2023. DOI: 10.1364/OPTICA.484200
- [8] D. Drayss, D. Fang, A. Sherifaj, H. Peng, C. Füllner, T. Henauer, G. Lihachev, L. Schmitz, T. Harter, W. Freude, S. Randel, T. J. Kippenberg, T. Zwick, and C. Koos, “Optical arbitrary waveform generation (OAWG) using actively phase-stabilized spectral stitching”, *Light: Science & Applications*, vol. 14, no. 1, p. 353, Sep. 2025. DOI: 10.1038/s41377-025-01937-4
- [9] S. Civelli, D. P. Jana, E. Forestieri, and M. Secondini, “A new twist on low-complexity digital backpropagation”, *Journal of Lightwave Technology*, vol. 43, no. 10, pp. 4679–4692, 2025. DOI: 10.1364/JLT.43.004679
- [10] R. Sohanpal, E. Sillekens, F. M. Ferreira, R. I. Killey, P. Bayvel, and Z. Liu, “On the Impact of Frequency Variation on Nonlinearity Mitigation using Frequency Combs”, in *Optical Fiber Communication Conference (OFC) 2023*, Optica Publishing Group, 2023, Th1F.3. DOI: 10.1364/OFC.2023.Th1F.3
- [11] A. A. I. Ali, F. Ferreira, M. Al-Khateeb, D. Charlton, C. Laperle, and A. D. Ellis, “The Impact of Dispersion Slope on Fiber Nonlinearity in Ultra-Wideband Optical Communication System”, in *2018 European Conference on Optical Communication (ECOC)*, Rome, Italy: IEEE, 2018. DOI: 10.1109/ECOC.2018.8535564
- [12] L. Galdino, D. Semrau, D. Lavery, G. Saavedra, C. B. Czegledi, E. Agrell, R. I. Killey, and P. Bayvel, “On the limits of digital back-propagation in the presence of transceiver noise”, *Optics Express*, vol. 25, no. 4, p. 4564, Feb. 2017. DOI: 10.1364/OE.25.004564
- [13] C. B. Czegledi, G. Liga, D. Lavery, M. Karlsson, E. Agrell, S. J. Savory, and P. Bayvel, “Digital backpropagation accounting for polarization-mode dispersion”, *Optics Express*, vol. 25, no. 3, pp. 1903–1915, Feb. 2017. DOI: 10.1364/OE.25.001903
- [14] C. R. Menyuk, “Nonlinear pulse propagation in birefringent optical fibers”, *IEEE Journal of Quantum Electronics*, vol. 23, no. 2, pp. 174–176, Feb. 1987. DOI: 10.1109/JQE.1987.1073206
- [15] O. V. Sinkin, R. Holzlohner, J. Zweck, and C. R. Menyuk, “Optimization of the split-step fourier method in modeling optical-fiber communications systems”, *Journal of Lightwave Technology*, vol. 21, no. 1, pp. 61–68, Jan. 2003. DOI: 10.1109/JLT.2003.808628
- [16] M. Kushnerov, F. Hauske, K. Piyawanno, B. Spinnler, M. Alfiad, A. Napoli, and B. Lankl, “DSP for Coherent Single-Carrier Receivers”, *Journal of Lightwave Technology*, vol. 27, no. 16, pp. 3614–3622, Aug. 2009. DOI: 10.1109/JLT.2009.2024963